Proceedings of the 11th World Congress on New Technologies (NewTech'25)
Paris, France - August, 2025
Paper No. ICCEIA 146
DOI: 10.11159/icceia25.146

Effects of Friction Coefficient on Movable Bearing Behaviour

Kota Dobashi[1], Yuichi Ito[1], Kouichi Takeya[1], Eiichi Sasaki[1]
[1]Institute of Science Tokyo
W6-7, 2-12-1 Ookayama, Meguro ward, Tokyo prefecture, Japan
dobashi.k.68e1@m.isct.ac.jp; ito.y.ca@m.titech.ac.jp; takeya.k.aa@m.titech.ac.jp; sasaki.e.ab@m.titech.ac.jp

Abstract **-** Movable bearings are expected to respond to bridge expansion and contraction due to temperature changes and train loads. However, due to the friction within a bearing, actual bearing movement tends to be smaller than theoretical prediction. This discrepancy between actual situation and theoretical evaluation can suggest that the girder expansion or contraction is constrained, thereby causing stresses and frictional reaction forces at the bearing seat. Although bearing friction is expected to increase with age, there is no standardized method for evaluating the friction coefficient, making it unclear when preventive maintenance actions should be implemented. This study aims to estimate the friction characteristics of bearings in actual bridges using finite element method (FEM) analysis and field measurements. The measurements have revealed a characteristic behavior whereby the bearings initially stick and then slip. This bearing behavior was then reproduced using numerical simulation, demonstrating the feasibility of estimating the friction coefficient of movable bearings under in-service conditions.

Keywords**:** *Bearing Friction, Friction Coefficient, Bearing Behavior, Temperature Change*

1. Introduction

Movable bearings are expected to respond to bridge expansion and contraction due to temperature change and train loads. However, Nishida et al. [1] and Shono et al. [2] show that the number of damaged shoe seat mortar is also not small, and such damage is most common in the line bearings. Nishida et al. [1] and Nara [3] show that the bearing's adherence worsens during the time it is in service. In fact, from Sugawara et al. [4], there is a case of adhered line bearings. In this case, the girder expansion and contraction became fixed by these adhered bearings and consequently the girder applied a force onto the bearings, causing them to move. Practically, Structural Design Office [5] states that damage to the shoe seats may occur due to sticking of the movable bearing.

Although bearing damage can occur during the maintenance phase due to bearing sticking, according to Structural Design Office [5], although qualitative assessments such as the degree of corrosion and wear, quantitative evaluation of such sticking has not been conducted, making it difficult to take specific countermeasures at the appropriate time. Niwa et al. [6] obtained friction coefficient of a movable bearing under in-service condition by determining the force in the direction of the bridge axis acting the bearing from the measured stress distribution in the girder and dividing it by the dead load acting on the bearing. Reading [6], it is considered that this method requires many measurement points because the stress distribution in the girder is not uniform.

This research aims to evaluate the bearing adhesion degree to contribute to decision-making in the maintenance phase. First, the movement of bearings under temperature change, which is considered to be affected by the bearing friction coefficient, was investigated using actual measurements and analysis. Based on these results, the possibility of estimating friction coefficients for in-service bridges has been demonstrated. To establish a more versatile method, this research has further explored a method to derive the friction coefficient by focusing on the movement of the bearing, which requires only one measurement point.

2. Field Measurements on Actual Bearing Behavior

2.1. Target Bridge

To investigate bearing movement caused by temperature change or the passage of a train, measurements were conducted on Kikugawa Bridge along the Tokaido Shinkansen line. The target span of the bridge is shown in **Fig.1** and a general view of the bridge is shown in **Fig.2**.

Fig.1 Kikugawa bridge target span

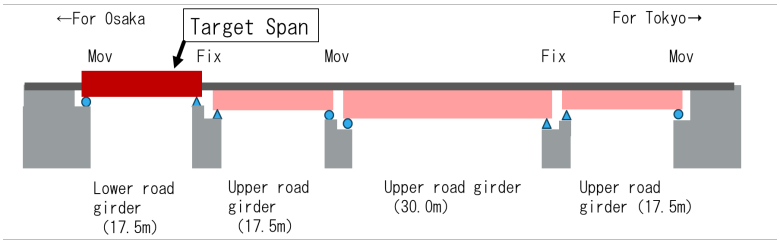

Fig.2 General view of Kikugawa bridge

Fig.3 The situation of measurement

The target bridge consists an open-floor, through which a separate plate girder bridge with three main girders and two tracks passes. The span length of the target section is 17.5 m. Continuous welded rails are used in this section, and there are no rail joints within the target span. Since its opening in 1964, the target bridge has undergone several reinforcements and soundproofing upgrades. The bridge employs line bearings, as shown in **Fig.3**, which were recently replaced as part of maintenance activities. The bridge experiences frequent train passage during daytime hours. However, no commercial trains operate between 0:00 and 6:00, and only maintenance vehicles pass.

2.2. Temperature-Bearing Displacement Relationship

The temperature-displacement relationship of the target bridge was measured over a four-day period as shown in **Fig.4**. The member temperature was measured near the movable bearing of the central girder, and the bearing displacement was measured at the movable bearing on the northern side of the three main girders. The displacement was considered positive in the direction of girder expansion. The location of the displacement meter is also shown in **Fig.3**. The displacement

transducer used was either a PI-type (Tokyo Measuring Instruments Laboratory Co. Ltd. PI-5-50) or a contact-type (Tokyo Measuring Instruments Laboratory Co. Ltd. CDP-50), where a coin-type thermos-hygrometer was used as the thermometer.

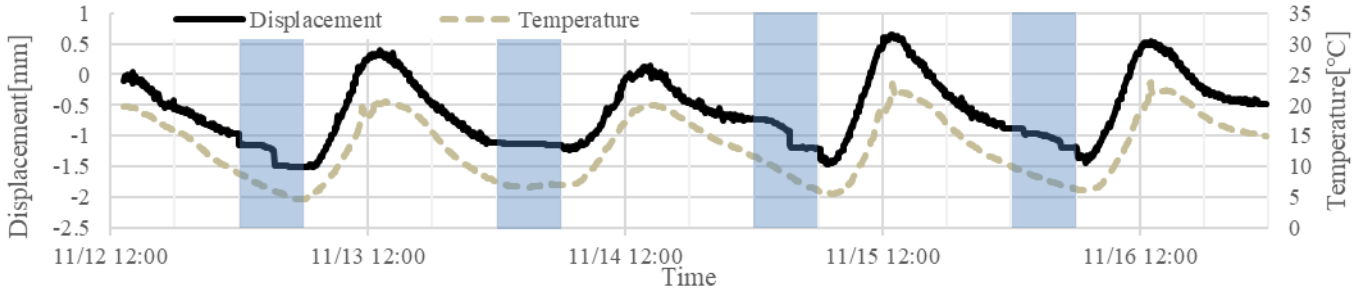

Fig.4 Displacement and temperature in measurement period

In **Fig.4**, the shaded sections indicate late-night hours between 0:00 and 6:00. **Fig.4** shows that although bearing displacement generally changes in response to temperature changes between 6:00 and 24:00 on each day, it remains in contact, decreases gradually, or changes abruptly during the late-night hours between 0:00 and 6:00. We focus on each of these two curves.

2.3. Bearing Movement During Daytime

Firstly, bearing movements during daytime hours between 6:00 and 24:00 were considered as during this period, many commercial trains pass. The waveform shown in **Fig.5** represents the bearing displacement when a train passes.

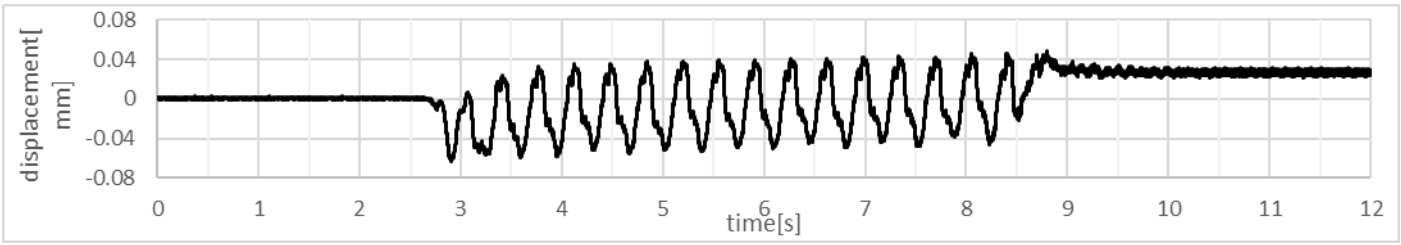

Fig.5 Bearing displacement during train passage

Niwa et al. [6] pointed out that the change in the horizontal displacement of the bearings before and after the train passage indicates that the friction-constrained thermal expansion and contraction of the bearings is released by the train passage. During the daytime, the trains passing impact cause bearing displacement, and the bearing is considered to follow the temperature change of the girder with small increments of movement as in Niwa et al. [6].

2.4. Bearing Movement During Late-Night Hours

Next bearing movements during late-night hours between 0:00 and 6:00 were considered. During this period, the bearing displacements either fluctuated abruptly or remained constant initially and then gradually decreased. These characteristic movements are shown in **Fig.6**, where the measurements were recorded on 16 November.

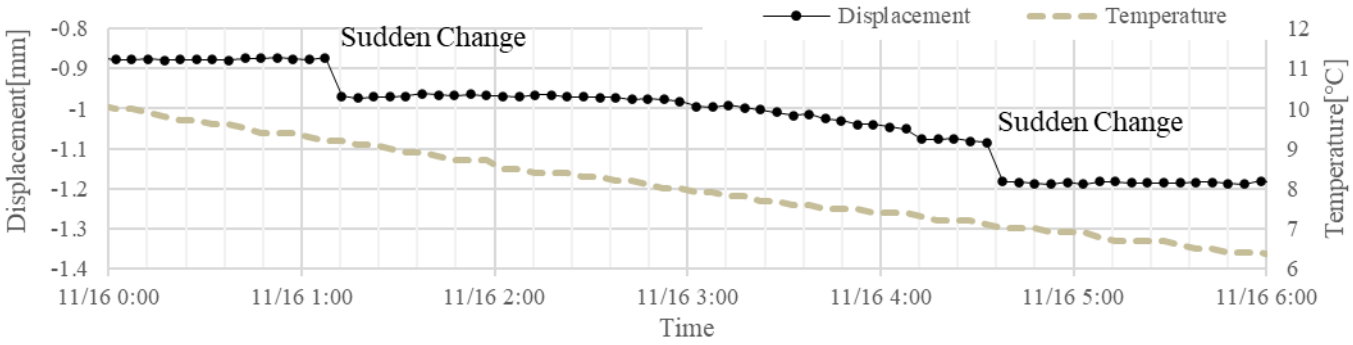

Fig.6 Bearing movement in late-night

The sudden change observed in bearing displacements in **Fig.6** is considered to have occurred due to the passing of a maintenance vehicle, which abruptly releases previously restrained displacements. For the latter movement, although the test was conducted for different type of bearing from Kikugawa Bridge, Nishida et al. [1] conducted loading tests on bearings and showed that the behavior of static and dynamic friction appears when stainless steel slides against each other. Therefore, the bearings did not move due to the absence of frequent impacts from commercial trains passing during late-night hours. However, under decreasing temperatures and when the thermal tensile axial force of the girder reached maximum static frictional force of the bearing, bearings started to slide, causing the displacement to gradually decrease. **Fig.7** shows an example of such a case, which occurred during the night of 16 November, the same day as the experiment conducted for **Fig.6**.

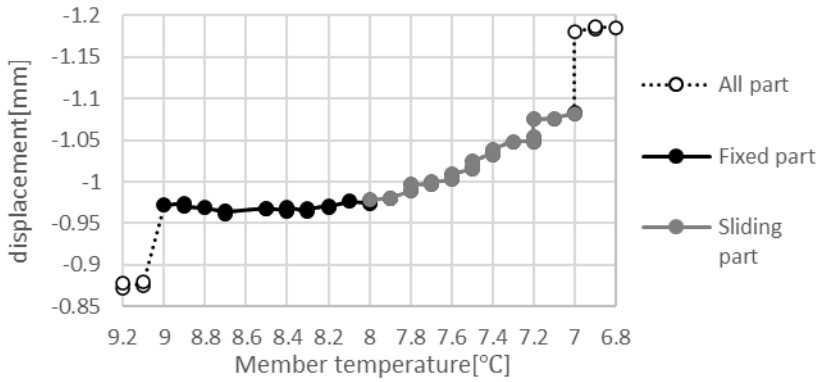

Fig.7 Temperature and displacement relationship by measurements

The thermal tensile axial force of the girder acting on the bearings were considered to be proportional to temperature changes. When the bearing started to slide, it was considered to be balanced by the maximum static friction force. In other words, the temperature range between when the bearing begins to adhere and when it starts to slide should be proportional to the friction coefficient.

Thus, it was found that the bearings generally followed the temperature during the daytime. However, the effect of bearing friction became apparent during the nighttime. FEM analysis of the target bridge was conducted to reproduce the bearing movements shown in **Fig.7** and determine the coefficient of proportionality between the bearing friction coefficient and temperature range.

3. Consideration Bearing Behavior using FEM Analysis

FEM analysis was conducted to reproduce the bearings movements shown in **Fig.7** and to investigate the relationship between the friction coefficient and temperature change.

3.1. Model Settings

The overall bridge model used for analysis is shown in **Fig.8**. Abaqus 2017 software was used for analysis. The target bridge features line bearings, constructed in the model as shown in **Fig. 9**. The movable bearing side includes a contact element, while the fixed bearing side features a fixed contact element between the bottom shoe and the sole plate. Bearing friction was modeled using the Lagrange multiplier method between the bottom shoe and the sole plate of the movable bearings.

Boundary conditions were set at the underside and backside of the abutments, the underside of some ballasts, and at the rail ends. The boundary conditions restricted displacement and rotation in all directions for the underside and backside of the abutments, displacement in all directions for the underside of the ballasts, and displacement in the rail axial direction for the rail ends. The piers were reproduced; however, their dimensions did not match the original specifications. The continuous welded rail, lower lateral bracing, and brake truss were also reproduced.

The material parameters used for analysis are shown in **Table 1**. The stiffness of both the members connecting the lower lateral bracing to the longitudinal girders and the brake truss were sufficiently increased to suppress deformation. The rail linear expansion coefficient was set to zero.

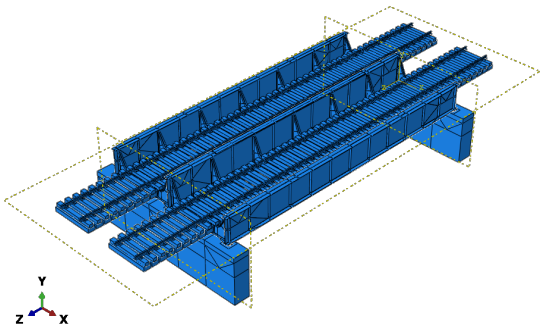

Fig.8 Panoramic view of analysis model

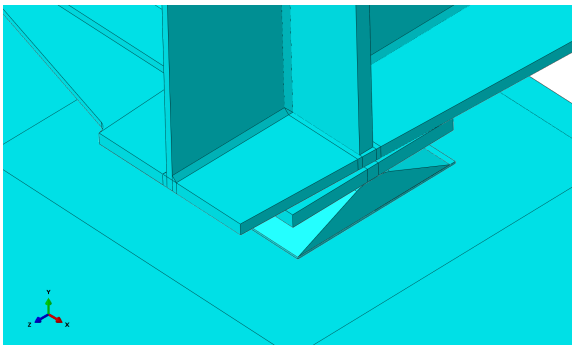

Fig.9 Model of line bearing

Table 1 Material parameters

	steel	concrete	ballast
Elastic Modulus[N/mm²]	200000	35000	111
Poisson's Ratio	0.3	0.17	0.17
Linear Expansion Coefficient [10^{-5}/°C]	1.2	1.2	1.2
Density[g/cm³]	7.85	2.35	-

3.2. Loading Condition

The effect of the movable bearing friction on the constrained thermal expansion and contraction of the girder was then examined. In this analysis, the bridge was loaded with its own weight and a friction coefficient was applied on the movable bearings. Next, the temperature of the bridge members was uniformly increased. A total of three cases was initially analyzed, where the friction coefficients of the movable bearings were set to 0.2, 0.5, and 0.8.

The analysis reproduced bearing movement during the late-night period as there are no commercial trains in this period and train loads can be excluded.

3.3. Temperature and Displacement Relationship

Fig.10 illustrates the relationship between the rise in temperature of bridge members and the relative displacement between the bearing and the sole plate along the bridge axial direction for each analysis. The displacements were extracted from two points near the tangent line between the sole plate and the lower shoe in the side girder bearing; namely the inner and outer points, perpendicular to the bridge axis. Initially, no displacement was observed, however, after the temperature reached a certain threshold, displacement increased in an approximately linear manner. The thermal load of the girder due to the restrained expansion and contraction of the girder is assumed to have exceeded the maximum static friction force of the movable bearing, causing the bearings to move.

Fig.10 shows a similar behavior to **Fig.7** as the bearing displacement initially remains constant before increasing or decreasing linearly from a certain temperature. Therefore, we can estimate the friction coefficient from the measured temperature ΔT, where the bearings begin to slide, by comparing with the analysis result.

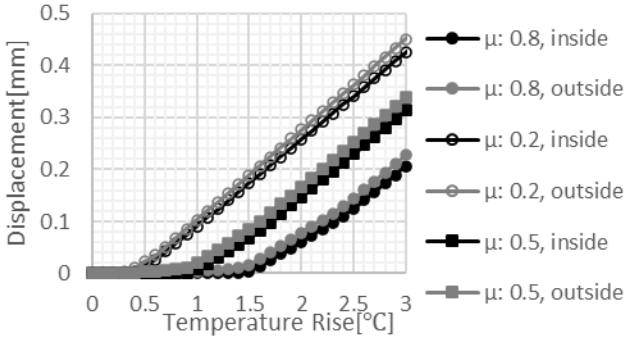

Fig.10 Temperature and relative displacement relationship

3.4. Difference due to Friction Coefficient

The relationship between the temperature at which the bearings begin to slide (denoted as ΔT) and the friction coefficient (denoted as μ) is shown in **Fig.11**. Linear approximation of the friction coefficient μ and temperature ΔT results in $\Delta T = 1.8602\mu$ (referred to as Eq. (1)), with an R-squared value of 0.9994.

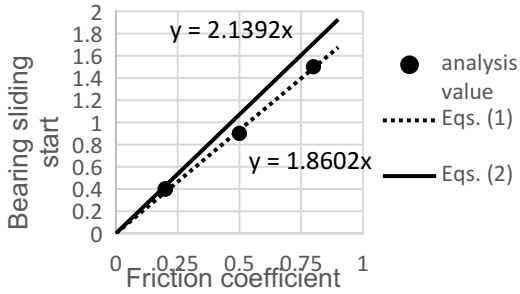

Fig.11 Relationship between friction coefficient and bearing sliding start temperature

Therefore, there is a strong correlation between the friction coefficient μ and the temperature ΔT when the bearings begin to slide. This suggests that the friction coefficient of the bearings can potentially be assessed.

Considering the formula based on the bending theory of beams, an equation for the relationship between the temperature ΔT and the friction coefficient μ was derived in a simplified manner.

In this equation, the cross-sectional area of the girder is represented as A, the modulus of elasticity is denoted as E, the sectional secondary moment is represented by I and the coefficient of linear expansion is expressed as α. The dead weight acting on the bearing is referred to as w and the distance between the point where the friction force is applied and the neutral

axis of the girder is denoted by l. The cross-sectional area of the girder is assumed to be equal to the minimum cross-sectional area. The dead weight acting on the bearings is calculated as 7.74×10^4[N], which is obtained by distributing the weight of the analytical model with considering vertical stresses in the bearings. The vertical stresses does not completely include the weight of the members connecting the lower lateral bracing to the longitudinal girders and brake trusses. Nonetheless, this effect is expected to be negligible.

The main girder is subjected to a bending moment of $lw\mu$ by the maximum static friction force just before the bearings begin to slide. Since the bearings are sticking, the displacement is zero at the underside of the sole plate, and the girder strain on the underside of the sole plate remains equal to the thermal expansion strain of $\alpha \Delta T$. Applying the bending theory of a simply supported beam, we obtain Eq. (2) as below.

$$\Delta T = \frac{l^2 w}{IE\alpha}\mu = 2.14\mu \quad (2)$$

Fig.11 also shows the relationship between the friction coefficient μ and the temperature ΔT using Eqs. (1) - (2). Eq. (2) calculated the temperature ΔT to be 15.0% higher than the analytical Eq. (1).

3.5. Difference due to Continuous Welded Rail

The effect of continuous welded rails has also been considered in this study. According to Railway Technical Research Institute [7], the continuous welded rail constrains the girder expansion and contraction, which affects the movement of the bearings. **Fig.12** shows the movements at the bearing center points. One is based on a friction coefficient of 0.5, and the other is observed when the stiffness of the continuous welded rail, brake truss, and lower lateral bracing decreases to 200 MPa for the same model (denoted as 'no continuous welded rail model').

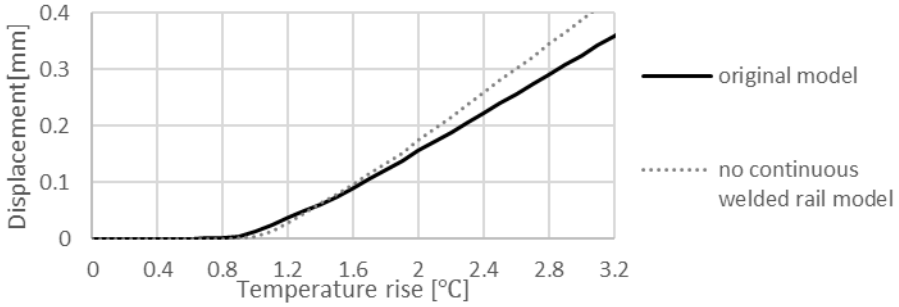

Fig.12 Displacement of original model and model without continuous welded rail (displays discrete data as a polyline)

In **Fig.12**, the temperature at which bearings start to slide slightly increased for the model without continuous welded rails. Regarding the slope of the bearing displacements during bearing sliding, the original model showed a smaller slope compared to the model without continuous welded rails, which is considered to be due to the restraint applied to the bridge girder from the continuous welded rail.

4. Conclusion

This study shows that it is potentially feasible to estimate the friction coefficient by considering the movement of a bearing under temperature change, which can enhance bridge maintenance efficiency. The findings are summarized as follows:

(1) Field measurements have shown that under frequent train passage, bearings move in response to temperature change, whereas under less frequent train passage frictional effects prevail and the bearing does not move. Bearing movements resulted in gradual displacement after sticking during infrequent train passages. This suggests that the friction coefficient can be estimated from bearing behavior.

(2) The analysis conducted in this study shows that during temperature change, the movable bearings remain initially stationary then begin to slide once the absolute temperature change reaches a specific threshold. A strong correlation therefore exists between the absolute temperature change during bearing sticking and the friction coefficient.

This research attempts to estimate the friction coefficient of the bearing; however, the accuracy remains uncertain. Enhancing the accuracy of friction coefficient estimations remains a challenge to be considered in future studies.

Acknowledgements

We would like to thank Mr. Hirai of Central Japan Railway Company for his assistance with conducting field measurements and analysis in this study.

References

[1] H. Nishida, M. Kimura, F. Yamada, T. Furuichi, S. Matsui, “Development of replacement bearing in steel railway bridge,” *Journal of Structural Engineering*, JSCE, vol. 65A, pp. 419-431, March, 2019.

[2] I. Shono, Y. Yamada, S. Matsui, "A database for the damage near the bearing support," *Proceedings of Annual Conference of the Japan Society of Civil Engineers*, Vol. 49, Division 1, pp. 342-343, 1994.

[3] I. Nara, “[Support structures of steel railway bridges],” *Structural Design Data*, no. 4, Japanese National Railways, pp. 132-139, 1965. (in Japanese)

[4] T. Sugawara, H. Onishi, M. Satomi, “Estimation of bearing movement status and quantitative evaluation of restraint status in road bridge behavior measurement,” *Journal of the Society of Materials Science*, Japan, vol. 71, no.3, pp. 303-309, March, 2022.

[5] Bureau of Facilities, Structures Design Office, [*Guideline for Repair of Steel Railway Bridge Bearings*], December, 1984, pp. 5-11, 17, 21. (in Japanese)

[6] Y. Niwa, S. Yajima, Y. Takahashi, K. Komon, “Behavior of the bearings with bearing plate of the railway composite girder bridge used for 38 years and evaluation of axial force acting on the bearings,” *Journal of Structural Engineering*, JSCE, vol. 64A, pp. 421-434, March, 2018.

[7] Railway Technical Research Institute, [*Design Standards and Commentary for Railway Structures: Steel and Composite Structures*], Maruzen Co., Ltd., October, 1992, pp. 19, 22-23, 32-34, 40, 46-47, 55-56, 91-98, 224-226. (in Japanese)